INDIAN JOURNAL OF SCIENCE AND TECHNOLOGY

RESEARCH ARTICLE

Enhancing the Degradation of All Moieties of the Environment Pollutant Congo Red Dye in Dark, White Light, and Solar Light by using CuS Nanoflowers: A Quantita tive Analysis

Sampa Mondal[1], **Baibaswata Bhattacharjee**[2]*

1 Department of Physics, Bankura Zilla Saradamani Mahila Mahavidyapith, Bankura University, Bankura, 722101, West Bengal, India
2 Department of Physics, Ramananda College, Bankura University, Bankura, 722122, West Bengal, India

OPEN ACCESS

Received: 20-05-2024

Accepted: 11-07-2024

Published: 06-08-2024

Citation: Mondal S, Bhattacharjee B (2024) Enhancing the Degradation of All Moieties of the Environment Pollutant Congo Red Dye in Dark, White Light, and Solar Light by using CuS Nanoflowers: A Quantita tive Analysis. Indian Journal of Science and Technology 17(31): 3190-3198. https://doi.org/10.17485/IJST/v17i31.1721

* **Corresponding author**.

baib23@gmail.com

Funding: None

Competing Interests: None

Published By Indian Society for Education and Environment (iSee)

ISSN
Print: 0974-6846
Electronic: 0974-5645

Abstract

Objectives: To enhance the degradation rate of all moieties (azo, naphthalene, and phenyl) of Congo Red (CR) dye by using CuS nanoflowers under darkness, white light, and solar light. **Method:** CuS nanoflowers are synthesized by employing a simple wet chemical method. The sample is characterized by its microstructural and optical properties. The CuS nanoflower is added to the CR solution to investigate the degradation efficiency of CuS nanoflower in dark and light. **Findings:** The sample shows significant absorption between 300 and 700 nm, followed by a quick reduction. This study is the first to show that a CuS nanoflower can act as both a catalyst and a photocatalyst to degrade all moieties of Congo Red (CR), an environmental pollutant, in dark and light. 100% degradation of all CR dye moieties takes place in 24 min, 36 min, and 52 min in the presence of solar light, white light, and darkness, respectively. When comparing experimental settings (consecutively darkness, white light, and solar light), the change in degradation efficiency for the azo, naphthalene, and phenyl moieties with time is the highest under solar light followed by white light and darkness in order. The reactions followed pseudo-first-order kinetics according to the Langmuir-Hinshelwood (L-H) model. The degradation rate for all moieties of CR is the highest under solar light irradiation, lower under white light irradiation, and lowest in darkness. Additionally, CuS nanoflowers exhibit exceptional recyclability. **Novelty:** The phenyl moiety of CR is degraded 100% in dark and light. Additionally, the degradation rate of all moieties is enhanced due to the greater surface area of nanoflowers. To the best of our knowledge, the present study is the first one to report that the CuS nanoflower synthesized in this work can act as both a catalyst and a photocatalyst to degrade all moieties of Congo Red (CR), an environmental pollutant, in darkness and light.

Keywords: CuS nanoflowers; Photocatalyst; Catalyst; 100% CR degradation; Rate of degradation efficiency.

1 Introduction

Copper sulfide nanoparticles (NPs) are often found in five crystalline polymorphs: chalcocite (Cu_2S), djurleite ($Cu_{1.95}S$), digenite ($Cu_{1.8}S$), anilite ($Cu_{1.75}S$), and covellite (CuS)[1]. However, CuS NPs are a p-type semiconducting material that has gained popularity among researchers due to its low band gap energy (1.63-1.87 eV), size, shape, versatility, availability, stability, and non-toxic nature. As a result, CuS NPs are used in several applications such as chemical sensors, switches, optical filters, energy conversion, and storage[1].

The total yearly manufacture of synthetic dyes is more than 7,000 tons. Textile waste effluents leak about 15% of non-biodegradable dyes into natural streams and water bodies each year[2]. Highly colored dyes hinder light penetration and negatively disrupt biological processes in streams. Furthermore, in anaerobic reduction circumstances, azo dyes easily produce aromatic amines, which are more dangerous. Therefore, eliminating these physically unpleasant and poisonous colors from wastewater is essential for protecting aquatic life from their harmful effects. Because of this, multiple investigations on dye degradation have been conducted utilizing various nanoparticles that reduce the adverse effects of dyes[3]. In this sense, it is very important to increase the degradation efficiency of CuS NPs.

Several studies have shown that CuS has excellent photocatalytic activity. This has prompted research into developing synthesis routes for CuS particles with different sizes, shapes, and morphologies, as these factors significantly impact photocatalytic performance[1]. Lately, some efforts have been made in CR dye degradation studies using different nanoforms of copper sulfide[4]. However, these investigations cannot degrade the phenyl moieties of CR dye. To entirely reduce the toxic effects of CR dye, all of its components (azo, naphthalene, and phenyl) must be completely degraded.

In recent years, many efforts have been made in experimental studies focusing on CR dye degradation using different nanostructures. For instance, Abumousa et al.[5] have reported that TiO_2/Y_2O_3@g-C_3N_4 can degrade 100 % of CR dye, and Gadore et al.[6] have reported $NiCo_2S_4$/chitosan nanocomposite can degrade 93.46% of CR dye solution. Furthermore, these investigations are limited to only visible light irradiation. It has been seen that $MgAL_2O_4$ NPs can degrade 99.27% of CR[7] and the nickel-titanium dioxide nanoflakes can degrade CR under UV light irradiation[8]. In these studies, nanostructures cannot degrade CR dye under darkness, visible light, and solar light irradiation. The research findings of Aldaghri et al.[9] show that $CaMgO_2$@g-C_3N_4 nanocomposite can decolorize 99% of CR solution and the investigation findings of Rianjanu et al.[10] show that cerium dioxide nanorods exhibit 97.7% CR degradation efficiency under UV illumination. In these investigations, $CaMgO_2$@g-C_3N_4 nanocomposite and cerium dioxide nanorods show photocatalytic activity only under UV illumination. To the best of our knowledge, there are no experiments that have shown 100% degradation of all CR moieties within a very short time under darkness, visible light, and solar light irradiation.

CuS architectures have been described in many forms[4]. The photocatalytic and catalytic activity of NPs is primarily determined by their specific surface area and material quality[4]. So, flower-shaped morphologies have garnered substantial attention. In this study, a simple low-cost wet chemical technique is adopted for the synthesis of CuS nanoflowers, with better light sensitivity. The photocatalytic and catalytic activity of produced CuS nanoflowers in degrading all moieties of CR dye has been investigated. As far as we are aware, this is the first report on the dual role (catalyst and photocatalyst) of CuS nanoflower for the degradation of all components (azo, naphthalene, and

phenyl) of environmental pollutant CR under darkness, white light, and solar light. CuS nanoflowers have high catalytic and photocatalytic efficacy due to their wide surface area and small band gap. In both dark and light, each reaction is shown to follow pseudo-first-order kinetics according to the Langmuir–Hinshelwood (L–H) model. Furthermore, the XRD pattern, FESEM image, and UV-Vis spectra of CuS nanoflower do not change significantly after the 6th cycle of dye degradation, demonstrating that CuS nanoflowers are recyclable. This work reveals that CuS nanoflower can effectively be used for photocatalytic and catalytic degradation in wastewater treatment and environmental remediation.

2 Methodology

2.1. Materials and Methods

Cupric acetate monohydrate (Sigma-Aldrich, purity 99.99%) and sodium thiosulphate pentahydrate (Sigma-Aldrich, purity 99.99%) are utilized as precursors without further purification. To begin, 22.5 mmol of Copper acetate monohydrate (Cu $(CH_3COO)_2.H_2O$) is dissolved in 250 mL of deionized (DI) water (Merck, purity 99.99%) (concentration= 0.0175 g/mL) while vigorously stirring at room temperature. Separately, 26.2 mmol of sodium thiosulphate pentahydrate ($Na_2S_2O_3.5H_2O$) is dissolved in 250 mL of DI water (concentration= 0.0250 g/mL), followed by stirring at room temperature. The $Na_2S_2O_3.5H_2O$ solution is then dropped into the Cu $(CH_3COO)_2.H_2O$solution, and the resulting green-black solution is stirred continuously for 4 hours at 90°C. The precipitates are then obtained by filtering this green-black solution by Whatman no 1 filter paper and being rinsed five times with DI water. After being rinsed, the precipitates are dried at 120°C in a hot air oven for 4 hours. Finally, the subsequent product is pulverized to produce fine CuS powder.

2.2. Characterizations and Instrumentation

A Bruker D8 Advance diffractometer has been utilized for assessing CuS NPs' crystallinity across an angle range (2θ) of 20–80°. The morphology of the synthesized sample is investigated using a Zeiss Sigma field-enhanced secondary electron microscope (FESEM). Using a Jasco V-770 spectrophotometer, UV-VIS absorption spectra between 200 and 1000 nm in wavelength are collected.

2.3. Catalysis and photocatalysis for degradation of CR

Degradation experiments are conducted in a Pyrex conical flask (100 mL). The CR solution of 100 ppm is prepared by adding approximately 0.01 g CR in 100 mL DI water. A 0.04 g CuS nanoflower is allowed to react with a 100 mL dye solution. The pH of the final solution is adjusted at pH 7 (using 0.1 N HCl or 0.1 NaOH). The photocatalytic activities are estimated by exposing this solution to solar light (average intensity is 100000 lux) and white light (200 watts, average intensity is 1600 lux and wavelength range of 400-700 nm), while the adsorption ability of CuS nanoflowers is examined in the dark. A syringe is used to collect 2 mL of sample from each set and the dye concentration of each sample is examined by spectrophotometer after every certain time interval. These time intervals for the set under darkness, white light, and solar light are 4-minute, 3-minute, and 2-minute respectively. The UV-Vis spectrophotometer is scanned from 200 to 1000 nm and the wavelength with maximum absorptions at 495 nm, 350 nm, and 230 nm are monitored.

3 Results and Discussion

3.1. X-ray diffraction (XRD)

The XRD spectra of CuS NPs is shown in Figure 1. The XRD patterns in Figure 1 show wide peaks, implying the nano nature of the sample. The sample exhibits the peaks located around $2\theta^\circ$ positions of 27.67°, 29.27°, 31.87°, 32.81°, 47.95°, 52.67°, 59.42°, 74.03° which are attributed to the crystal planes 101, 102, 103, 006, 110, 108, 116, 208 respectively, confirming the hexagonal crystal structure of the CuS NPs[11]. The average size of the CuS NPs can be estimated by applying the Debye-Sherrer formula and the following equation:[12–15]

$$D = \frac{0.89\,\lambda}{\beta\, COS\theta} \tag{1}$$

where the Bragg angle is θ, the full width at half maximum (FWHM) is β, the x-ray wavelength is λ, and the shape factor is 0.89. The mean particle size of CuS NPs is 10 nm.

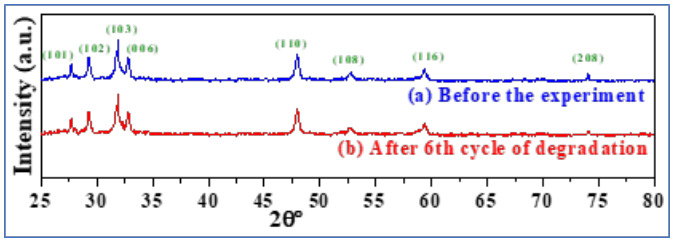

Fig 1. XRD patterns of CuS NPs: (a) before the experiments, (b) after the 6th cycle of degradation

3.2. Morphological Investigation

The morphological dimensions of CuS NPs can be investigated with the use of FESEM images (Figure 2**a).** The majority of CuS NPs have an oval or spherical shape. Figure 2**a** (inset) shows the particle size distribution histograms obtained from this FESEM image. Based on the FESEM image, the average particle size of CuS NPs is 9.5 nm. Figure 2 **a** shows that CuS nanoflower consists of an aggregation of many NPs with a mean particle size of 9.5 nm. A temperature of 120°C promotes the homogeneous formation of CuS crystalline nuclei and then these CuS NPs are self-assembled to generate CuS nanoflower.

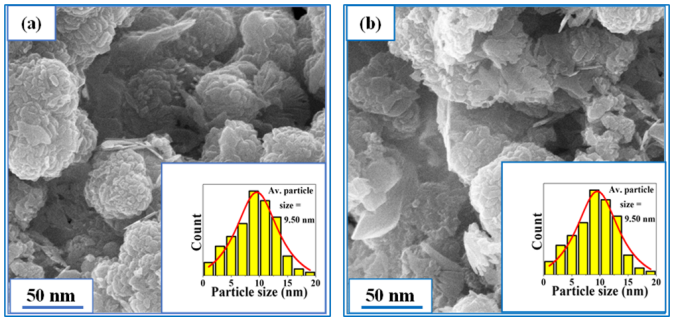

Fig 2. FESEM image with corresponding particle size distribution histograms of CuS NPs: (a) before the experiments, (b) after the 6th cycle of degradation

3.3. UV-VIS spectroscopy

The optical properties of CuS Nanoflowers are assessed using UV-vis spectroscopy. The absorption spectra of CuS nanoflower is shown in Figure 3. In this research, the sample exhibits a significant absorption between 300 and 700 nm, followed by a quick reduction (Figure 3). CuS NPs absorb light at wavelengths <700 nm due to indirect interband transitions[16]. This observation can be ascribed to the fact that the sample can absorb UV rays and visible rays. Hence, CuS nanoflower is a promising photocatalytic material. The energy gap E_g can be calculated by assuming a straight transition between the valance band and the conduction band. Based on the theory of optical absorption, the relationship between the absorption coefficient α and the photon energy hv for direct allowed transition can be interpreted as follows:[17–19]

$$(\alpha h\nu)^2 = A(h\nu - E_g) \quad (2)$$

Where A relates to the index of refraction and the effective masses of holes and electrons. The direct band gap is computed by extending the straight component of the $(\alpha hv)^2$ against hν plot, also called the Tauc plot, to cross the energy axis at α=0. The estimated band gap of NPs is 1.75 eV. Furthermore, a band extending into the near-IR region can be seen (Figure 3), which is indicative of CuS[16].

3.4. Measurement of catalytic and photocatalytic activity

Despite the absence of hydrogen peroxide, CuS nanoflowers are found to degrade the dye both photo-catalytically and catalytically in the current investigation. For adsorption to occur equilibrium, the CuS Nanoflowers and dye combination is left for an entire night. It's interesting to observe that the solution becomes colorless without changing the suspended CuS

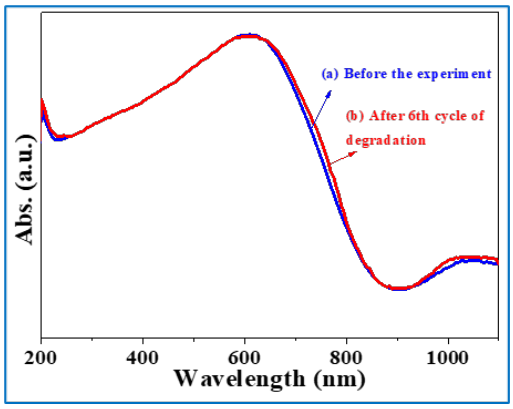

Fig 3. UV-VIS absorption spectrum of CuS nanoflower: (a) before the experiments, (b) after the 6th cycle of degradation

nanoflower's color, indicating its catalytic function. For this reason, a time-dependent experiment is conducted in complete darkness. The UV-Vis spectra of CR, as seen in Figure 4a, have three peaks that correspond to the moieties of azo (495 nm), naphthalene (350 nm), and phenyl (230 nm). Throughout the dark period, the absorption intensities of these peaks decrease steadily, and after 52 minutes, full degradation is seen (Figure 4 **a**). Cu-vacancies/holes on the surface can act as electron scavengers/acceptors, making CuS nanoflowers a p-type semiconducting material[4]. CuS nanoflowers exhibit catalytic activity due to surface defects and broken bands, resulting in surface energy states in the material's band gap[4].

In the presence of white light and solar light, full degradation of all moieties of CR dye is achieved in 36 min (Figure 4**b**) and 24 min (Figure 4 **c**) respectively. Under solar light irradiation, CuS nanoparticle electrons from the conduction band are promoted to the valence band due to their appropriate band gap (1.75 eV). As a result, dye is degraded by holes and electrons through oxidative and reductive processes, respectively. Similar phenomena occur under white light irradiation[4].

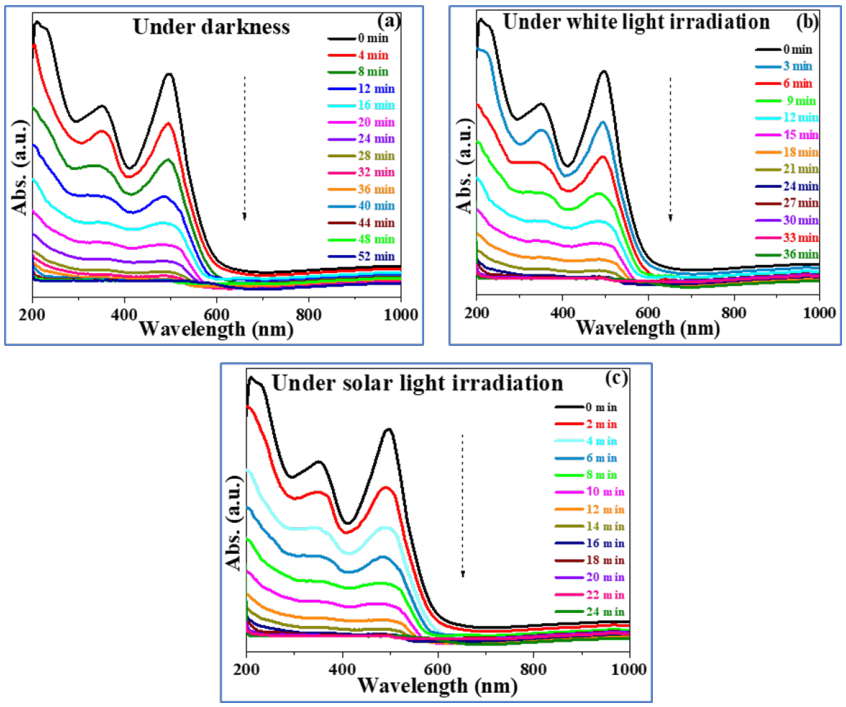

Fig 4. Time-dependent absorption spectral changes of all moieties of CR by CuS nanoflowers under (a) darkness, (b) white light irradiation, and (c) solar light irradiation

3.4.1. Time-dependent degradation efficiency

The Beer-Lambert law is used to generate a calibration plot of absorbance vs concentration. The degradation efficiency is determined using the following formula:[20] [21–23]

$$Degradation\ efficiency\ (\%) = \left[1 - \frac{C_t}{C_0}\right] \times 100 \tag{3}$$

The concentrations of CR at zero time and after time t (min) are denoted by C_0 and C_t respectively. 100% degradation efficiency of CuS nanoflower under darkness, white light, and solar light is seen at 52 min, 36 min, and 24 min respectively.

Figure 5**a, c**, and **e** show that the degradation efficiency for azo, naphthalene, and phenyl moieties exhibit a progressive change when the experimental conditions vary and or the experimental time changes. The degradation efficiency for azo, naphthalene, and phenyl moieties of CR increases with time for each experimental case. The changes in degradation efficiency for azo, naphthalene, and phenyl moieties with time under various experimental conditions (darkness, white light irradiation, and sunlight irradiation) are well fitted with the exponential growth scheme according to Equations (4), (5) and (6) respectively:

$$A(t) = (A)_f - \psi_A e^{(-t/\tau)} \tag{4}$$

$$N(t) = (N)_f - \beta_N e^{(-t/\mu)} \tag{5}$$

$$P(t) = (P)_f - \xi_P e^{(-t/\eta)} \tag{6}$$

Where, A(t), N(t), and P(t) are changes in degradation efficiency for azo, naphthalene, and phenyl moieties respectively with time (t). Here, $(A)_f$,$(N)_f$, and $(P)_f$ are the asymptotic degradation efficiency for azo, naphthalene, and phenyl respectively. "Asymptotic degradation efficiency for azo", "asymptotic degradation efficiency for naphthalene" and "asymptotic degradation efficiency for phenyl" are understood quantitively to be the degradation efficiency for azo, naphthalene, and for phenyl respectively at the last time of each experimental case (A→$(A)_f$, N→$(N)_f$, and P→$(P)_f$ as t→∞). Moreover, τ, μ, and η are growth constants; ψ_A,β_N, and ξ_P amplitude of exponentially growth values of degradation efficiency for azo, naphthalene, and phenyl respectively. Furthermore, low values of τ, μ, and η mean A(t), N(t), and P(t) increase more with t, respectively. In addition, high values of ψ_A,β_N, and ξ_P mean A(t), N(t), and P(t) increase more with t, respectively. The values of τ, μ, and η are shown in Figure 5**a, c**, and **e** respectively. In this study, the $(A)_f$,$(N)_f$, and $(P)_f$ for each case is 100%.

The decreasing order of τ values from 12 to 5.34, and increasing order of ψ_A values from 103.06 to 104.28 with varying experimental conditions (consecutively darkness, white light, solar light) attributed that A(t) increases in descending order when exposed to solar light, white light, and darkness (Figure 5**a**). Similarly, changing the experimental settings (as mentioned before) resulted in lowering μ values from 12.94 to 6.06 and rising β_N values from 108.19 to 108.92, pointing to the fact that the N(t) is the highest under solar light irradiation followed by white light and darkness in order (Figure 5**c**). In addition, when comparing experimental conditions (as mentioned above), the decreasing order of η values from 12.94 to 6.03 and the rising order of ξ_P values from 104.19 to 106.95 suggested P(t) increases in decreasing order when exposed to solar light, white light, and darkness (Figure 5 **e**). However, the degradation efficiency of CuS nanoflowers is greater under solar light irradiation than white light irradiation because they may absorb both UV and visible rays from sunlight.

3.4.2. Degradation kinematics studies

The L-H model is utilized to illustrate CR degradation kinetics.

$$ln\left[\frac{C_0}{C_t}\right] = kt \tag{7}$$

In this equation, t represents the reaction time and the apparent pseudo-first-order reaction rate (k) is constant which is derived from the slope[24,25]. As per the L–H model, the degradation process follows pseudo-first-order kinetics in both the presence and absence of a light source. The values of k for azo, naphthalene, and phenyl moieties are shown in Figure 5**b, d**, and **f** respectively.

The increasing order of k values for azo moiety from 0.128 to 0.281 with changing experimental conditions consecutively from darkness to white light and then to solar light indicates that the degradation rate for azo moiety is the greatest under solar

light irradiation followed by white light and darkness in order (Figure 5**b**). Again, when the experimental settings are changed (as previously noted), the order of k values for the naphthalene moiety increases from 0.114 to 0.250, implying the degradation rate for naphthalene moiety is the highest under solar light irradiation, lower under white light settings and lowest in darkness (Figure 5**d**). Once more, in the above-mentioned comparison of experimental circumstances, the rising order of k values for the phenyl moiety from 0.108 to 0.238 revealed the degradation rate for phenyl moiety is the highest under solar light followed by white light and darkness in order (Figure 5 **f**). Compared to the other moieties, the azo moiety is degraded most rapidly in both dark and light.

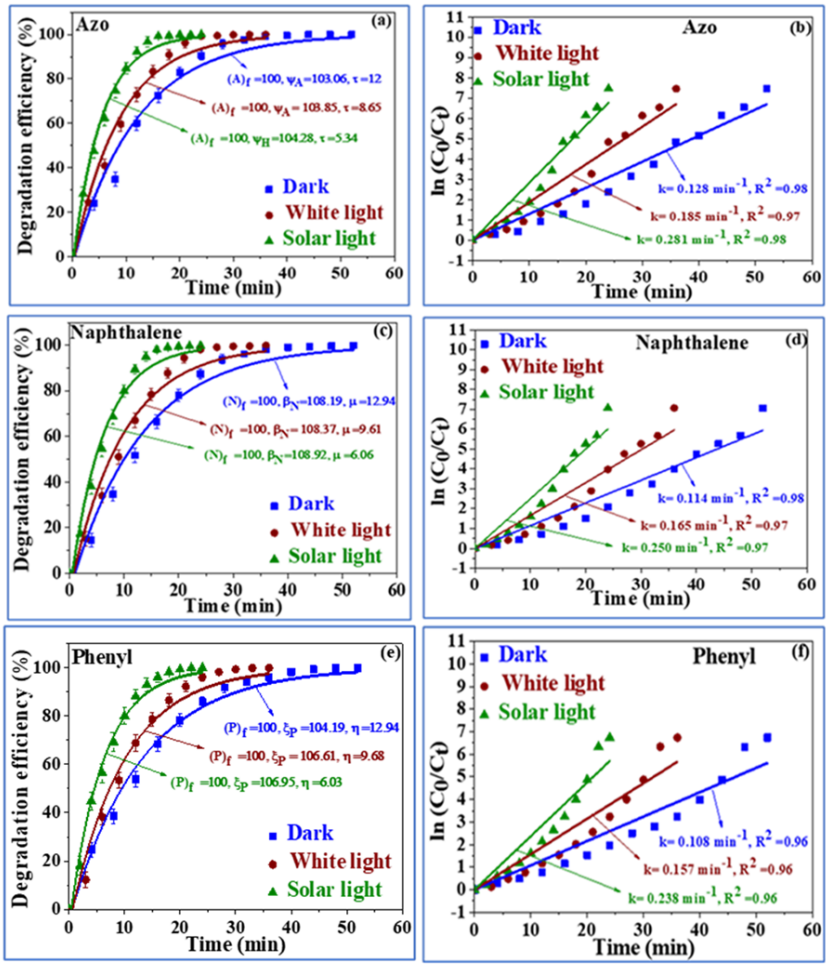

Fig 5. Time-dependent degradation efficiency for all CR moieties, their corresponding pseudo-first-order kinetics of degradation under different experimental settings: (a, b) azo moiety, (c, d) naphthalene moiety, (e, f) phenyl moiety

It has been reported that photocatalyst CuS NPs (30 mg/mL dye solution) can degrade 60.35 % of CR dye (dye concentration = 13.93 mg/L deionized water) in 240 min [4]. In this study, it has been possible to degrade CR dye only in light. In another research, Cu_2S nanocrystals have the capacity to degrade CR dye (dye concentration= 0.36 mg/L deionized water) in 135 min [4]. According to this study, this nanocrystal has 80% degradation efficiency in light and 15% degradation efficiency in the dark. As per the findings of Ain et al., both in dark and light, CuS nanoplates (0.5 mg/mL dye solution) can fully degrade azo and naphthalene moieties of CR dye (dye concentration= 100 mg/L deionized water) [4]. This study shows only azo and naphthalene moieties of CR dye are degraded 100% at 40 min in solar light and 80 min in the dark. These investigations show that the phenyl moieties of the CR dye cannot be degraded. On the other hand, Abumousa et al. [5] have reported that TiO_2/Y_2O_3@g-C_3N_4 can completely degrade CR dye within 60 min, and Gadore et al. [6] have found that a nanocomposite consisting of $NiCo_2S_4$/chitosan can degrade 93.46% of the 35 ppm CR dye solution in 60 minutes. Moreover, the scope of these studies is restricted to irradiation with visible light alone. It has been shown that when exposed to UV light, $MgAL_2O_4$ NPs can

degrade 99.27% of the CR dye (dye concentration= 25 mg/L deionized water) in 80 minutes [7] and that nickel-titanium dioxide nanoflakes can degrade CR dye [8]. These investigations show that $MgAL_2O_4$ NPs and nickel-titanium dioxide nanoflakes cannot degrade CR dye in the presence of darkness, visible light, and solar light irradiation. The study results of Rianjanu et al. [10] demonstrate that cerium dioxide nanorods exhibit 96.7 % CR degradation efficiency within 130 min, while the research results of Aldaghri et al. [9] show that $CaMgO_2$@g-C_3N_4 nanocomposite can decolorize 99% of CR solution (rate constant = 0.07 min-1). In these studies, the $CaMgO_2$@g-C_3N_4 nanocomposite and cerium dioxide nanorods exhibit photocatalytic activity specifically under UV light irradiation.

Compared to the previous reports, the CuS nanoflowers are superior in four arenas: they can degrade 100% of all CR moieties, a very small quantity of CuS nanoflowers is required for 100 % degradation, they have high photocatalytic degradation capability even under white light irradiation, and they have high degradation rate in dark and light. The remarkable performance of nanoflowers can be attributed to their large contact area due to their tiny size and flower-shaped morphology, which efficiently adsorbs CR and triggers deterioration due to unsatisfied valences on the surface.

3.4.3. Recyclable nature of CuS nanoflower

Six cycles of degradation process are conducted to ensure CuS nanoflower's stability. The findings show that CR is almost 100% degraded in all cycles. Additionally, CuS nanoflowers exhibit no extra peak in the XRD pattern after 6 cycles (Figure 1), only the intensity of peaks decreases slightly, indicating the same phase of CuS NPs after the 6^{th} cycle. The particle size distribution from the FESEM image of CuS nanoflowers remains unchanged after 6 cycles, only the surface of nanoflowers becomes slightly smooth due to being in the liquid medium for a long time (Figure 2 **b**). The absorption spectra of nanoflower also after 6 cycles cover the total UV and visible region and the band gap remains unaltered (Figure 3). These barely noticeable changes seen following the 6th cycle are insignificant and have no impact on the CuS nanoflower's degrading efficiency, confirming its recyclable nature.

4 Conclusion

A simple and eco-friendly wet chemical technique is used to synthesize CuS nanoflowers. Photocatalytic and catalytic study reveals that CuS nanoflowers show superior activity towards the 100% destruction of all moieties of CR dye. In the presence of solar light, white light, and darkness, 100% degradation of all CR dye moieties occurs in 24 min, 36 min, and 52 min, respectively. When comparing the experimental settings, the maximum values of τ, μ, and η are found under solar light irradiation. In light and dark, the reaction is found to follow pseudo-first-order kinetics as stated by the L–H model. The degradation process is fastest in the presence of sunlight (k=0.281 min^{-1} for azo, k=0.250 min^{-1} for naphthalene, and k=0.238 min^{-1} for phenyl). The azo moiety degrades most rapidly in both dark and light. Regarding the degradation of CR, the CuS nanoflower also shows outstanding stability, reusability, and recyclability. Therefore, CuS nanoflowers can be efficiently utilized in the remediation of environmental issues and wastewater streams by eliminating organic dye CR. The excellent dye degradation of CR by CuS nanoflowers can reduce the harmful effects of the dye on aquatic life and ecosystems. The breakdown of CR dye has made water safer to use in industry and to drink.

To remove dangerous colours and contaminants from wastewater, CuS nanoflowers are employed in the textile, dyeing, and printing sectors. CuS nanoflowers may be added to water treatment systems to eliminate colors and organic contaminants, producing clean water for a range of uses. By breaking down dyes and pollutants, CuS nanoflowers can be utilized to clean up polluted groundwater and soil. The textile sector may lessen its environmental effect by using CuS nanoflowers to produce eco-friendly and sustainable dyeing methods. With potential applications in various sectors, the use of CuS nanoflowers in wastewater treatment offers a viable, long-term option for environmental restoration.

CuS nanoflowers will be used to degrade the CR dye for a short time or will be used intermittently. So, the leaching of copper from CuS can be prevented while maintaining high catalytic performance. The process more intense, like centrifugal partitioning or microchannel reactors may enhance the efficiency of CuS nanoflowers. Changes like doping or composite production can enhance performance, stability, and recyclability. Integrating CuS photocatalysis with other procedures such as electrochemistry or membrane separation may increase the scalability and efficacy of CuS photocatalyst and its applications in continuous flow reactors.

Acknowledgment

The authors would like to acknowledge the Co-ordinator, Centre of Excellence in Advanced Materials, National Institute of Technology Durgapur, for microstructural characterization.

References

1) Mahanthappa M, Kottam N, Yellappa S. Enhanced photocatalytic degradation of methylene blue dye using CuS CdS nanocomposite under visible light irradiation. *Applied Surface Science*. 2019;475:828–866. Available from: https://doi.org/10.1016/j.apsusc.2018.12.178.
2) Nisansala HMD, Rajapaksha GKM, Dikella D, Dheerasinghe MJ, Sirimuthu NMS, Patabendige CNK. Zinc Oxide Nanostructures in the Textile Industry. *Indian Journal of Science and Technology*. 2021;14(46):3370–95. Available from: https://doi.org/10.17485/IJST/v14i46.1052.
3) Kumar R, Umar A, Kumar G, Akhtar MS, Wang Y, Kim SH. Ce-doped ZnO nanoparticles for efficient photocatalytic degradation of direct red-23 dye. *Ceramics International*. 2015;41(6):7773–82. Available from: https://doi.org/10.1016/j.ceramint.2015.02.110.
4) Ain NU, Zia-Ur-Rehman, Aamir A, Khan Y, ur MR, Lin DJ. Catalytic and photocatalytic efficacy of hexagonal CuS nanoplates derived from copper(II) dithiocarbamate. *Materials Chemistry and Physics*. 2020;242:122408–122408. Available from: https://doi.org/10.1016/j.matchemphys.2019.122408.
5) Abumousa RA, Bououdina M, Aissa MAB, Khezami L, Modwi A. Efficient photocatalytic degradation of Congo red and other dyes by ternary TiO2/Y2O3@g-C3N4 nanohybrid. *Journal of Materials Science: Materials in Electronics*. 2024;35(7):486–486. Available from: https://doi.org/10.1007/s10854-024-12264-6.
6) Gadore V, Singh AK, Mishra SR, Ahmaruzzaman M. RSM approach for process optimization of the photodegradation of congo red by a novel NiCo2S4/chitosan photocatalyst. *Scientific Reports*. 2024;14(1). Available from: https://doi.org/10.1038/s41598-024-51618-.
7) Al-Farraj ES, Abdelrahman EA. Efficient Photocatalytic Degradation of Congo Red Dye Using Facilely Synthesized and Characterized MgAl2O4 Nanoparticles. *ACS Omega*. 2024;9(4):4870–4880. Available from: https://doi.org/10.1021/acsomega.3c08485.
8) Indira K, Shanmugam S, Hari A, Vasantharaj S, Sathiyavimal S, Brindhadevi K, et al. Photocatalytic degradation of congo red dye using nickel-titanium dioxide nanoflakes synthesized by Mukia madrasapatna leaf extract. *Environmental Research*. 2021;202:111647–111647. Available from: https://doi.org/10.1016/j.envres.2021.111647.
9) Aldaghri O, Alqarni L, Modwi A, Idriss H, Abumousa R, Ali M, et al. Efficient photodecolorization of Congo red by CaMgO2@g-C3N4 nanocomposite. *Journal of Materials Science: Materials in Electronics*. 2024;35(7):478–478. Available from: https://doi.org/10.1007/s10854-024-12232-0.
10) Rianjanu A, Mustamin ASP, Melati E, Aflaha R, Khamidy NI, Utami M, et al. Photocatalytic degradation of aqueous Congo red dye pollutants by rare-earth metal oxide (CeO2) nanorods. *Colloids and Surfaces A: Physicochemical and Engineering Aspects*. 2024;682:132919–132919. Available from: https://doi.org/10.1016/j.colsurfa.2023.132919.
11) Iqbal S, Shaid NA, Sajid MM, Javed Y, Fakhar-E-Alam M, Mahmood A, et al. Extensive evaluation of changes in structural, chemical and thermal properties of copper sulfide nanoparticles at different calcination temperature. *Journal of Crystal Growth*. 2020;547:125823–125823. Available from: https://doi.org/10.1016/j.jcrysgro.2020.125823.
12) Chevva S, Tirumalareddygari SR, Guddeti PR, Kotte TRR. Precursor Molarity Influence on Sprayed Mo-doped ZnO Films for Solar Cells. *Indian Journal of Science and Technology*. 2022;15(36):1800–1807. Available from: https://doi.org/10.17485/IJST/v15i36.842.
13) Ansari SA, Parveen N, Alsulaim GM, Ansari AA, Alsharif SA, Alnahdi KM, et al. Emerging NiO-rGO nanohybrids for antibiotic pollutant degradation under visible-light irradiation. *Surfaces and Interfaces*. 2023;40:103078–103078. Available from: https://doi.org/10.1016/j.surfin.2023.103078.
14) Ansari SA. Elemental semiconductor red phosphorus/ZnO nanohybrids as high performance photocatalysts. *Ceramics International*. 2023;49(11):17746–52. Available from: https://doi.org/10.1016/j.ceramint.2023.02.140.
15) Sheth MN, Shukla V. Photocatalytic decolorization of mercuric picrate in the presence of zinc oxide. *Indian Journal of Science and Technology*. 2020;13(15):1589–95. Available from: https://doi.org/10.17485/IJST/v13i15.134.
16) Sood S, Umar A, Mehta SK, Kansal SK. Highly effective Fe-doped TiO 2 nanoparticles photocatalysts for visible-light driven photocatalytic degradation of toxic organic compounds. *Journal of Colloid and Interface Science*. 2015;450:213–236. Available from: https://doi.org/10.1016/j.jcis.2015.03.018.
17) Sahu D. Synthesis of Cerium doped Zinc oxide nanoparticles by aqueous precipitation method and study on the structural and optical properties. *Indian Journal of Science and Technology*. 2020;13(14):1480–1485. Available from: https://dx.doi.org/10.17485/ijst/v13i14.337.
18) Kansal SK, Lamba R, Mehta SK, Umar A. Photocatalytic degradation of Alizarin Red S using simply synthesized ZnO nanoparticles. *Materials Letters*. 2013;106:385–389. Available from: https://dx.doi.org/10.1016/j.matlet.2013.05.074.
19) Kansal SK, Sood S, Umar A, Mehta SK. Photocatalytic degradation of Eriochrome Black T dye using well-crystalline anatase TiO2 nanoparticles. *Journal of Alloys and Compounds*. 2013;581:392–397. Available from: https://dx.doi.org/10.1016/j.jallcom.2013.07.069.
20) Ait-Karra A, Zakir O, Mourak A, Elouakassi N, Almaggoussi A, Idouhli R, et al. Elaboration of CuS nanomaterials via hydrothermal route: Examining physical properties and photocatalytic potential. *Journal of Physics and Chemistry of Solids*. 2024;185:111771–111771. Available from: https://doi.org/10.1016/j.jpcs.2023.111771.
21) Kumar R, Kumar G, Umar A. ZnO nano-mushrooms for photocatalytic degradation of methyl orange. *Materials Letters*. 2013;97:100–103. Available from: https://dx.doi.org/10.1016/j.matlet.2013.01.044.
22) Leela S, Gouthami M, Jayapriyan KR, R S. Photocatalytic Dye Degradation Potential of Silver Nanocomposite from Exo-polysaccharide of Bacillus sp., An Associative Bacterium of Sargassum wightii. *Indian Journal Of Science And Technology*. 2024;16(47):4481–4489. Available from: https://doi.org/10.17485/IJST/v16i47.1760.
23) Sood S, Umar A, Mehta SK, Kansal SK. α-Bi2O3 nanorods: An efficient sunlight active photocatalyst for degradation of Rhodamine B and 2,4,6-trichlorophenol. *Ceramics International*. 2015;41(3):3355–3364. Available from: https://dx.doi.org/10.1016/j.ceramint.2014.10.038.
24) Amirtham PJM, Shenbhagaraman R, Siva R. Photocatalytic Dye Degradation and Bacteriostatic Efficacy of Myco Synthesized Copper Nanoparticles by new Isolate Lentinus squarrosulus (Mont.) from Dead Trunk of Nerium odourum. *Indian Journal Of Science And Technology*. 2023;16(24):1802–1809. Available from: https://doi.org/10.17485/IJST/v16i24.252.
25) Santbay L, Kassir M, Nassar R, Mokh S, Iskandarani MA, ARifai. Removal of benzophenone-4 via chlorination and advanced oxidation processes in aqueous solution: kinetics, by-product identification, and mechanistic studies. *Environmental Science and Pollution Research*. 2024;31(21):31201–31212. Available from: https://dx.doi.org/10.1007/s11356-024-33191-3.